A Simple Model of the Climatology and Variability of the Low-Level Wind Field in the Tropics*

RICHARD SEAGER

Lamont Doherty Geological Observatory of Columbia University, Palisades, New York

(Manuscript received 16 November 1989, in final form 30 August 1990)

ABSTRACT

A simple model of the low-level wind field in the entire tropics is presented. The dynamics are the same as those within the familiar Gill model, i.e., linear, steady state, contained within a single vertical mode and damped by Rayleigh friction. Convective atmospheric heating can occur if a lifted air parcel is buoyant relative to its surroundings, and the heating is computed with reference to the cloud model of Yanai et al. Radiative cooling is represented by a Newtonian cooling to an equilibrium lapse rate. The model is forced by surface temperature and humidity. A qualitatively correct representation of the climatological flow is achieved. The main differences between model and observations relate to the model's inability to reproduce the intensity and limited spatial scale of the convergence zones. Model simulations of anomalous circulations are subject to the same limitations. Problems related to the lack of an explicit boundary layer in the model, the poor representation of radiation, and the cumulus parameterization are discussed, together with suggestions for future work.

1. Introduction

A large amount of modeling in the last decade has been directed at the dynamical processes in the tropical atmosphere and ocean. Much of this work has been aimed at developing coupled atmosphere–ocean models that can be used to simulate, analyze, and perhaps predict the large interannual variability observed in the tropics. So far the main focus has been on the Pacific sector and the dynamics of El Niño (e.g., Zebiak and Cane 1987). Future problems that will have to be tackled include African and Brazilian drought and possibly monsoon variability.

In both the coupled models and nature, information flows from atmosphere to ocean via the winds and heat flux at the surface and from ocean to atmosphere via the sea surface temperature (SST). Much of our progress in understanding the coupled system has come about through modeling either the atmosphere or ocean given the forcing provided by the other medium. After Matsuno (1966) demonstrated the free-wave solutions to the linear equations of motion in the equatorial atmosphere, early attempts to model the atmosphere's response to imposed heating in areas of deep convection were made, with some success, by Webster (1972) and Gill (1980). More recently attempts to model the SST, given the observed winds as forcing, have been made by Philander and Siegel (1985), Latif (1987), Seager et al. (1988), Seager (1989), and Harrison et al. (1989), again with some success.

Gill's conceptual model was presented with the total flow over the tropical Pacific in mind. Webster (1972) and Neelin (1988) attempted to simulate the total response to atmospheric heating, and Neelin and Held (1987) modeled the divergent component of the total low-level wind based on a simplified moist static energy budget. With these exceptions, most efforts using simplified models have addressed anomalous circulations. This has yielded considerable insight into the tropical atmosphere–ocean system and has even been of practical use (most notably in the El Niño predictions of Cane et al. 1986). However it begs the question of why the climatology is what it is. Further, if anomalies in the oceanic and atmospheric fields interact nonlinearly with the mean, as seems likely, modeling the total fields will become unavoidable. Here, the Gill model is built upon to develop a simple model of the climatological low-level flow in the tropical atmosphere and then to look at its variability. Hopefully in the future a simple model of total atmospheric flow will be coupled to an ocean model similar to that of Seager et al. (1988) in order to analyze the atmosphere–ocean–land interactions that underlie the climatology and lead to variability.

Numerous attempts to model tropical flows have used approaches similar to that of Gill (1980). The attractiveness of the Gill model is its simplicity—it assumed that the flow was linear and contained within a prescribed vertical structure bounded by a level surface and an upper lid. Damping was provided by Ray-

* Lamont Doherty Geological Observatory Contribution 4716.

Corresponding author address: Dr. Richard Seager, Lamont Doherty Geological Observatory, Palisades, NY 10964.

leigh friction and Newtonian cooling. When forced with an imposed idealized heating, taken to represent latent heating in areas of deep convection, the model produced a circulation that bore more than a passing resemblance to that observed over the tropical Pacific. Neelin (1988) demonstrated that a similar model could be formulated in terms of boundary layer flow alone, thus justifying the large values of Rayleigh friction commonly used.

Zebiak (1982) used the same dynamical model but made the heating proportional to the observed SST anomalies associated with El Niño to again produce wind anomalies similar to those observed. Zebiak (1986) later included an additional heating term proportional to low-level convergence that was designed to mimic the CISK-type positive feedback effect of moisture convergence. Davey and Gill (1987) explicitly included a moisture equation and made the latent heating proportional to precipitation, which was allowed to occur when the humidity exceeded a certain amount.

Zebiak's and Davey and Gill's models, as well as others, each contain a convection parameterization that rests on the belief that moist convection occurs if the boundary layer approaches saturation. This produces a circulation with low-level moisture convergence in the region of heating, which causes more convection, thus intensifying the initial disturbance. Because these models implicitly assume that the atmosphere is conditionally unstable, this is a CISK-type process. Betts (1982) and Emmanuel (1986, 1989) have questioned whether the tropical atmosphere is in the mean conditionally unstable. Their argument, which in large part is accepted here, is that convection is forced by buoyancy and that while a high humidity will increase the buoyancy of boundary layer air, neither this nor moisture convergence is required for convection to occur.

Convection occurs if a raised air parcel is buoyant relative to its surroundings, and that could be so in the case of air with a low humidity or in a region of moisture divergence. Over the oceans the lifting condensation level is normally within a kilometer of the surface so it is not difficult to imagine turbulence in the absence of large-scale convergence, raising the air to saturation. Of course, once convection occurs the resulting circulation will force convergence in regions of convection so these two phenomena will normally be correlated. A positive feedback between circulation and convection is, however, still possible. Convection-induced convergence will increase the mass flux in clouds and the condensation. Because the atmospheric heating associated with convection is largely compensated by cooling due to mean adiabatic ascent (such that temperature does not change), the extra heating will require extra low-level convergence.

In the model presented here convection will be parameterized with reference to buoyancy and not explicitly to convergence. Atmospheric heating in regions of moist convection will be computed with reference to the cloud model of Yanai et al. (1973). This work also extends most previous work by considering the entire tropical zone and by modeling total winds, not just departures from climatology. To do this a crude representation of land processes will be used.

To attempt this with a simple dynamical model containing equally simple thermodynamics is a daunting task. By using the basic framework of the Gill model, however, numerous useful assumptions are built upon. The most significant of these is the use of a single vertical mode, which requires a midtropospheric maximum of atmospheric heating, as is observed in regions of convection. This bypasses the complex interplay of cloud processes and buoyancy forcing that achieves this vertical structure. Also, by forcing the model with surface temperature, the processes that determine this temperature are omitted.

Matters are further simplified by specifying the surface humidity from data. (Some preliminary attempts at computing it were far from encouraging over land areas.) While this constrains the model, it still has the freedom to determine its own latent heating field. Nonetheless, this is a weakness of the current model. It may well be, but so far has not been demonstrated, that humidity variations are an integral part of interannual variability. In the future a dynamic moisture equation will have to be included, but that problem is postponed for the moment.

As a further encouragement, the linear dynamics within the model have recently received justification from Zebiak (1990). Using observed winds and the vorticity equation, he demonstrated that the nonlinear terms were small compared with the linear terms and were smaller than the unexplained residual. He then "processed" observed winds through the Gill model to create a wind field and corresponding "apparent" heating field. The resulting winds were within the error range of the observed winds but now obeyed a dynamical balance that the observed winds did not. Further, the corresponding heating field looked physically realistic when compared to outgoing longwave radiation (OLR) data. The suggestion is that the difficulty of modeling tropical flows with simple models is to be found in the treatment of diabatic heating and not in the linear dynamics. Neelin's (1988) success in reproducing general circulation model (GCM) winds with a Gill-type model forced by GCM 700-mb pressure velocities or precipitation suggests the same conclusion.

The extensive use of the Gill model and its apparent successes raise the question of how it will perform in the more demanding situation here. We can learn from both its successes and failures. It will be argued that this simple model is capable of capturing many of the basic features of the tropical low-level wind field, that is deficiencies are explainable, and that it can provide insight into the relevant physics.

The next section describes the model, section 3 the

forcing data, section 4 the results of the climatological simulation, and section 5 the results of some simulations of anomalous circulations. Conclusions are presented in section 6.

2. The model

a. Dimensional equations

This development closely follows that of Davey and Gill (1987). The model describes perturbations around a state of rest with horizontally uniform surface temperature, lapse rate $d\theta_0/dz$, density $\rho_0(z)$, and pressure $p_0(z)$. Then the constant buoyancy frequency can be defined as

$$N^2 = (g/\theta_0)(d\theta_0/dz). \tag{1}$$

The atmosphere has a top at $z = z_T$ and a level bottom at $z = 0$ and is on an equatorial β-plane. The steady-state momentum equations with Rayleigh friction acting on a time scale ϵ^{-1} are

$$\epsilon u - fv = -p_x/\rho_0 \tag{2}$$

$$\epsilon v + fu = -p_y/\rho_0. \tag{3}$$

The continuity equation for incompressible flow is

$$u_x + v_y + w_z = 0 \tag{4}$$

and the thermodynamic equation is

$$wd\theta_0/dz = Q \tag{5}$$

where Q is the total heating including radiative and convective components. All other notation follows usual conventions.

The following vertical structure is assumed:

$$\mathbf{u} = \mathbf{u}'(x, y)\cos\pi z/z_T$$

$$w = w'(x, y)\sin\pi z/z_T$$

$$(Q, \theta) = [Q'(x, y), \theta'(x, y)](\theta_0/\theta_{00})\sin\pi z/z_T$$

$$p = p'(x, y)[\rho_0(z)/\rho_{00}]\cos\pi z/z_T.$$

Here θ_{00} and ρ_{00} are characteristic values of the potential temperature and density. Then with the approximate relation $(p/\rho_0)_z = g\theta/\theta_{00}$, we get, after dropping primes:

$$\epsilon u - fv = gz_T\theta_x/\pi\theta_{00} \tag{6}$$

$$\epsilon v + fu = gz_T\theta_y/\pi\theta_{00} \tag{7}$$

$$u_x + v_y + (\pi/z_T)w = 0 \tag{8}$$

$$wN^2\theta_{00}/g = Q. \tag{9}$$

b. Parameterization of atmospheric heating

There are four possible regimes that the atmosphere may locally be within depending on its stability to moist and dry convection. These will be associated with different forms of the atmospheric heating. First some thermodynamic parameters must be defined and evaluated.

It is assumed that the boundary layer potential temperature is approximated by the surface temperature (which is the SST over the oceans; over land it is in fact approximated by the surface air temperature anyway). This is a reasonable approximation except where there are large gradients of SST, such as in the Pacific equatorial cold tongue. Then since deviations from the mean surface pressure are small, the boundary layer potential temperature is about equal to the surface temperature. The atmosphere would be unstable to dry convection if the boundary layer potential temperature were greater than the midtroposphere temperature. In practice this never occurs, and this case is no longer considered.

The atmosphere will be unstable to moist convection if the equivalent potential temperature of the boundary layer air is greater than the equivalent potential temperature at saturation of the midtroposphere air. This assumes that all the condensate in rising parcels rains out. The equivalent potential temperature in the boundary layer is defined by

$$\theta_{eb} = \theta_b \exp(Lq/c_pT_c) \tag{10}$$

where L is the latent heat of condensation, θ_b is the total boundary layer potential temperature, c_p is the specific heat capacity of water, T_c is the temperature of the parcel after it has expanded adiabatically to saturation, and q is the water vapor mixing ratio. Using the fact that the mixing ratio is conserved in dry adiabatic ascent and that the relative humidity is known, T_c can be evaluated from tabulated values in the Smithsonian Meteorological Tables (List 1949). With this temperature, the boundary layer equivalent potential temperature can be evaluated everywhere from Eq. (10). In addition, the lifting condensation level, z_c, can be found from

$$z_c = (T_s - T_c)/0.0098 \text{ K m}^{-1} \tag{11}$$

where 0.098 is the value of the dry adiabatic lapse rate.

To compute the equivalent potential temperature at saturation of the midtroposphere, θ^*_{em}, the gross assumption is made that the saturation mixing ratio at this level is about zero such that

$$\theta^*_{em} = \theta_m = \theta_0(z_T/2) + \theta, \tag{12}$$

i.e., it is equal to the mean plus perturbation potential temperatures at this level. This assumption makes the model atmosphere more unstable to moist convection than should be the case. This error is compensated for somewhat by making the mean lapse rate of potential temperature slightly larger than observed.

With these thermodynamic properties, we can evaluate the atmosphere's stability to moist convection. The two possibilities are:

1) *Atmosphere stable to moist convection.* In this case no convection will occur, and only radiation will

contribute to the atmospheric heating. This is the case over colder ocean regions and drier land regions. Radiation is represented as a simple Newtonian cooling, damping the midtroposphere potential temperature perturbation θ on a time scale K^{-1} towards a radiative equilibrium temperature perturbation θ_s, which is calculated assuming an adiabatic lapse rate from the surface. This provides a radiative cooling everywhere. By assuming an adiabatic lapse rate, dry adiabatic adjustment is implicitly incorporated as an instantaneous process. Then Q is given by

$$Q = K(\theta - \theta_s). \tag{13}$$

2) *Atmosphere unstable to moist convection.* This is the more complicated case. The condition for this case is that the midtroposphere potential temperature, taken to approximate the equivalent potential temperature at saturation, is less than the boundary layer equivalent potential temperature and that the lifting condensation level is less than $z_T/2$. In practice the latter of these two conditions is rarely violated.

The parameterization of convective heating, Q_c, for this case is based on the cloud model of Yanai et al. (1973). Stevens and Lundzen (1978) used a similar parameterization in a wave-CISK model. Convective heating is composed of a turbulent transfer of sensible heat together with a net latent heat release and can be written

$$Q_c = Lc/c_p - d\overline{(\theta' w')}/dz \tag{14}$$

where c is the rate of condensation and the overbar denotes an average over the cloud and its environment. It has been assumed that the rate of reevaporation is small. Yanai et al. show that Eq. (14) can be written, if the lapse rate is approximated by the mean, as

$$Q_c = M_c d\theta_0/dz \tag{15}$$

where M_c is the cloud mass flux. Once the cloud mass flux is known, the convective heating is also known. The precipitation rate, P, must be given by the product of the cloud mass flux at the top of the boundary layer and the humidity of the boundary layer air carried up into the cloud if the cloud rains out all its moisture, which is probably not a bad approximation for these deep clouds. This can be written

$$P = M_c q. \tag{16}$$

If it is assumed that moisture is confined to the boundary layer, then, to conserve moisture in the boundary layer, the precipitation must be balanced by evaporation from the underlying surface and convergence of moisture. It is assumed that the mixing ratio of moisture is invariant at the value q across the depth of the boundary layer. The depth of the boundary layer is taken to be constant, and vertical shears of velocity within the layer are ignored. Then it is deduced that

$$M_c = P/q = (1/q)(E - z_B \nabla \cdot \mathbf{u}q) \tag{17}$$

where z_B is the depth of the boundary layer, and it is understood that precipitation cannot be negative.

The evaporation, E, is modeled using the familiar bulk formula

$$E = \beta\gamma(q_s - q) = \beta E_p. \tag{18}$$

E_p is the evaporation of a water surface, γ is an exchange rate, and β is the evaporation efficiency.

Equations (16)–(18) provide an estimate for the cloud mass flux appropriate to the cloud base. The heating derived from this and Eq. (15) need to be related to the assumed vertical structure. Yanai et al. (1973) show the heating to have a midtroposphere maximum and to be near zero at the surface and tropopause. The value of the heating given by Eq. (15) is therefore projected onto this mode, which introduces a multiplying factor of $\pi/2$. Radiation is modeled as before except that the Newtonian cooling is one-quarter of its clear-sky value. This reduction is designed to mimic the infrared absorption by clouds. The atmospheric heating is finally given by

$$Q = K(\theta - \theta_s) + (\pi/2q)M[(E - z_B \nabla \cdot \mathbf{u}q)]\frac{d\theta_0}{dz} \tag{19}$$

where the function $M[x]$ equals x for x greater than zero and is otherwise zero. This switch is included because the heating will be zero if P, as given by Eq. (17), is less than zero.

The atmosphere could locally occupy other regimes if a rising air parcel were not to saturate below midtroposphere level. In practice this never occurs.

It should be noted that the moisture balance of the boundary layer does not provide a self-consistent moisture or energy budget for the model. This is because the assumption of fixed humidity does not allow the moisture content to equilibrate with the changing convergence. The reference to moisture is included solely for the purpose of providing an estimate of the location and magnitude of convective heating. This approach is very different to the otherwise similar approach of Neelin and Held (1987) in that they computed tropical convergence beginning with a self-consistent moist static energy budget.

c. *Nondimensional equations*

Equations (6)–(9) and Eq. (19) are nondimensionalized with a length scale given by the equatorial Rossby radius, $a = (C/2\beta_0)^{1/2}$, which for a typical value of C of 60 m s^{-1} is around 1110 km. The time scale a/C is then about one-quarter of a day. The following nondimensionalization is used with asterisks denoting nondimensional values:

$$(x, y, z) = a[x^*, y^*, (z_T/a\pi)z^*]$$

$$(u, v, w) = C[u^*, v^*, (z_T/a\pi)w^*]$$

$$t = (a/C)t^*$$

$$(\theta, Q) = (C^2\theta_{00}\pi/gz_T)[\theta^*, (C/a)Q]$$

$$q = q^*$$

$$P = (Cz_T/a\pi)P^*$$

$$\gamma = (Cz_T/a\pi)\gamma^*$$

$$(\epsilon, K) = (C/a)(\epsilon^*, K^*).$$

Then the nondimensional system is, after combining Eqs. (8), (9), and (19) and dropping asterisks:

$$\epsilon u - yv/2 = \theta_x \tag{20}$$

$$\epsilon v + yu/2 = \theta_y \tag{21}$$

$$\nabla \cdot \mathbf{u} = -(\pi/2q)P + K(\theta_s - \theta) \tag{22}$$

$$P = \begin{cases} M[\beta\gamma(q_s - q) - z_B\nabla \cdot \mathbf{u}q], & \theta_{eb} > \theta^*_{em} \\ 0, & \theta_{eb} < \theta^*_{em} \end{cases}. \tag{23}$$

These equations are solved by an iterative method similar to that detailed in Zebiak (1986). Briefly Eqs. (20)–(22) are solved for the heating given by the right-hand side of Eq. (22), and then a new heating is computed from Eq. (23) to begin the next iteration. A stability analysis similar to that given by Zebiak (1986) shows that the scheme will converge if the dimensional boundary layer depth is less than 2500 m and the other components of the heating are finite and nonzero. Zebiak (1982) details the method of solution that involves combining Eqs. (20)–(22) into a single equation for v, fast Fourier transforming in x, spatial differencing in y, and solving the resultant tridiagonal system subject to the boundary condition that v is zero at 81°N and 81°S. The effective grid spacing is 5.625° in longitude and 2° in latitude. The model is only forced within ±29° of the equator.

3. Forcing data

The forcing is provided by surface temperature and water vapor mixing ratio. For air temperature above land the dataset compiled by Shea (1986) for the period 1950–79 is used. For the SST the Climate Analysis Center temperatures were used as described by Reynolds (1988). They cover the period January 1970 to August 1988 and include satellite derived SSTs after 1981. Because the model contains no treatment of topography in order to avoid abnormally cold surface temperatures in regions of high altitude, the temperature must be corrected to sea level. This was done by plotting the air temperature as a function of altitude using a topography dataset (G. Russell, personal communication) separately for Asia, Africa, and the Americas. Each continent was treated independently, as the lapse rate regimes were observed to be quite different. A lapse rate was estimated by eye for each region and used to adjust the surface temperature to sea level in any areas where the topography extended above 1000 m. The SST and land surface temperature datasets were then merged together. Where the two datasets joined they were smoothed by three passes of a 1–2–1 filter in both x and y. Figures 1a and 1b show the surface temperatures for the January and July climatologies.

The climatological surface mixing ratio is taken from the dataset of Oort (1983) covering the period 1958–73, which includes both radiosonde and surface station data. The fields for January and July are shown in Figs. 2a and 2b.

4. Results of the climatological simulation

The model contains a number of parameters that must be assigned values. These are given in Table 1. The Newtonian cooling coefficient corresponds to a relaxation time of about 25 days. The Newtonian cooling is reduced to one-quarter of the value given by this coefficient in regions of precipitation to mimic the effects of infrared absorption by clouds. The coefficient of Rayleigh friction gives a relaxation time of about 1.25 days. Such strong friction is only strictly valid for the boundary layer. The exchange coefficient for evaporation, β, equals the product of a drag coefficient and the wind speed if a bulk formula is assumed. If a typical wind speed of 6 m s^{-1} is assumed, the chosen value of the exchange coefficient corresponds to a drag coefficient of 0.0015 over the oceans and 0.0020 over land. This latter value is designed to account for the greater turbulence induced by a rougher surface. The efficiency of evaporation is 1 over the oceans. Over land this efficiency will be lowest in areas of little or no precipitation since the moisture availability is reduced. In wetter land areas it will be larger but still less than one since vegetation is capable of resisting moisture loss. Rather arbitrarily, the evaporation efficiency over land areas is assumed to be 0.8 where it is raining and 0.5 if it is not. Finally the dimensional boundary layer (which enters solely for the purpose of computing the cloud mass flux from the moisture equation) is 2000 m, and the depth of the troposphere is 15 000 m.

Figures 3a and 3b show the observed and modeled winds and divergence for the January climatology. The observed winds are from Oort (1983). Many of the large-scale features of the observed circulation are simulated by the model. The South Pacific convergence zone (SPCZ) is quite well represented, being only a little too weak, but the strength of the intertropical convergence zone (ITCZ) in the east and central Pacific is severely underestimated. Otherwise much of the flow over the Pacific is well captured including the turning of the winds over the maritime continent.

The model develops a heat source over the Amazon basin, but the associated wind field is quite wrong. The observed winds here appear to be highly influenced by heating over Panama and the eastern Pacific ITCZ, such that the winds blow to the west through the basin.

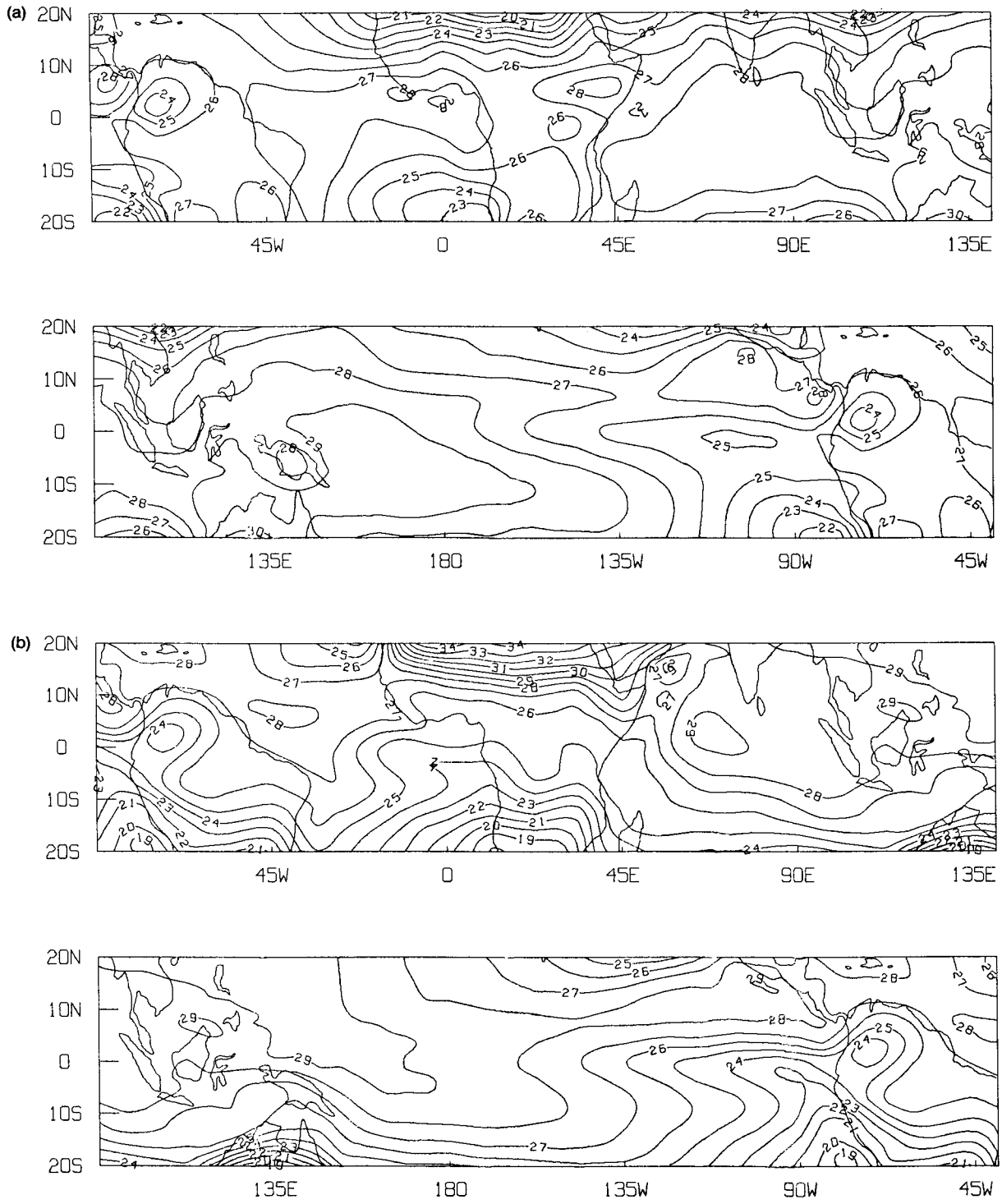

FIG. 1. Observed surface temperature (°C) for (a) January and (b) July climatology. Data are from Reynolds (1988) and Shea (1986).

In the model, the Panama–East Pacific heat source is underestimated and there is a region of divergence over the northern Andes separating this heat source from that over the Amazon. This is certainly a problem caused by the exclusion of the dynamic influence of topography and incorrect adjustment of the surface temperature to sea level. The Atlantic sector ITCZ is in the correct position but is too weak, and the con-

vergence over Africa does not have the areal extent that the observations indicate. Over the Indian Ocean the monsoon circulation is quite well modeled with a broad ITCZ covering most of the ocean. There is northeasterly flow from the Indian subcontinent in both model and observations turning into a westward flow near the equator. However, the model westerly flow is much too strong.

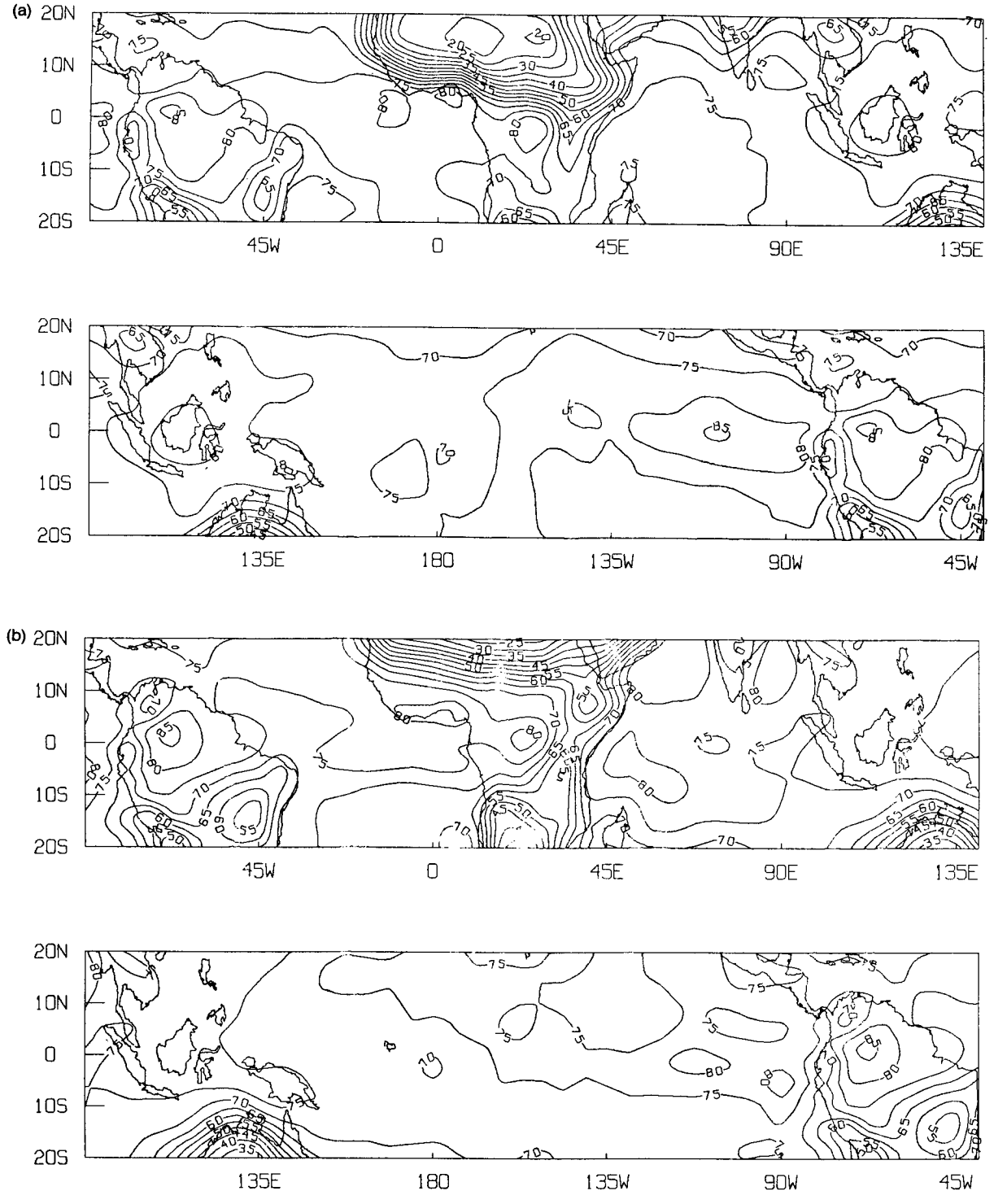

FIG. 2. Observed surface relative humidity (%) for (a) January and (b) July climatology. Data are from Oort (1983).

TABLE 1. Parameter values.

Rayleigh friction	$\epsilon = 0.2$
Newtonian cooling	$K = 0.01$
Exchange coefficient	$\gamma = \begin{cases} 0.0015, & \text{over ocean} \\ 0.0020, & \text{over land} \end{cases}$
Evaporation efficiency	$\beta = \begin{cases} 1.0, & \text{over ocean} \\ 0.8, & \text{over land and raining} \\ 0.5, & \text{over land not raining} \end{cases}$
Boundary layer depth	$z_B = 2000$ m
Troposphere depth	$z_T = 15\,000$ m

Figures 4a and 4b show the simulation and observations for the July case. Many of the same problems are evident as in January. The east Pacific ITCZ is again too weak, though correctly positioned, but the convergence zone in the west Pacific has about the right strength and has moved north in accord with observations. Underestimation of convergence over Panama and the problem associated with the Andes have again caused incorrectly directed flow over the Amazon. The Atlantic ITCZ is too broad in the correct position, but over Africa the region of convergence is too strong and narrow. The reversal of the monsoon circulation over the Indian Ocean has been well simulated with the exception of the intense East African jet. This feature is not expected to be captured since its location and strength are dictated by the presence of the East African highlands (Findlater 1969). However, the westerly winds north of the equator are again much too strong. The westerly flow over the northern Indian Ocean is far too strong and extends too far east over Southeast Asia. The Central American monsoon flow is misrepresented in a quite similar way with westerly flow over the Central American isthmus where it should be easterly.

In both months the model winds are too strong and too zonal. In addition, the model fails to create the small-scale structure that is evident in much of the observations (especially in the east Pacific ITCZ).

It is often stated that the linear dynamics contained within these models provide an incorrect representation of the zonal mean flow (see for example, Neelin 1988). A glance at the zonal momentum equation shows that the zonal mean zonal wind must be identically zero on the equator, whereas in nature there are weak zonal mean easterlies throughout the year that must be maintained by nonlinear effects. Other features of the zonal mean surface winds are actually quite well represented in the model, however. The main errors are trades that are too strong in the winter hemisphere, the development of spurious weak westerlies around 10°N in July, and a general tendency for the winds to be too zonal.

This model, in common with similar models, is quite sensitive to the values of the parameters chosen. For example, lowering the coefficient of Rayleigh friction not only increases the wind speed but also makes the winds more zonal. This also has the effect of further weakening the divergence. The magnitude of the divergence and wind speed can also be decreased by reducing the depth of the boundary layer. Reducing the radiative relaxation time to 12.5 days decreases the strength of oceanic, relative to continental, convergence zones. This is an artifact of the radiative equilibrium temperature being greater and, hence, radiative cooling less, over the warm land areas than over the oceans. The radiative cooling is overwhelmed by convective heating when the more realistic 25-day radiative relaxation time is used in the experiments presented here. No reasonable parameter changes reduce the spatial scale of the convergence zones.

Even with the reservations mentioned above it is clear that the model simulation captures much of the flow. The precipitation field (not shown) also has a pattern similar to that observed and indeed compares quite favorably with simulations by considerably more complicated models. Generally the results add weight to claims that the effect of nonlinear dynamics on the low-level flow is limited.

5. Simulation of anomalous circulations

Calculations were performed to analyze the model's ability to simulate some nonclimatological conditions. To do this the Climate Analysis Center's SST anomaly (SSTA) values, described by Reynolds (1988), for January 1987 and July 1988 were added to the climatological SST. These two months represent 1) the warm phase of the moderate 1986–87 El Niño and 2) a cold phase in the equatorial Pacific together with a warm event in the equatorial Atlantic. Climatological surface humidity was used everywhere so the only anomalous forcing was the SSTAs.

Figure 5 shows the SST anomaly for January 1987. Figure 6 shows the 1000-mb wind anomalies taken from the National Meteorological Center (NMC) analysis (see Trenberth and Olson 1988 for a discussion of this analysis) together with the negative of the OLR anomaly (see Gruber and Krueger 1984). Here, and in the second case, the wind anomalies are relative to a monthly climatology for the period May 1986 to December 1989. Figure 7 shows the model wind and precipitation anomalies for the same period.

Not surprisingly, the model captures the westerly wind anomalies in the central Pacific. In the model these are centered on the equator rather than just south of the equator as seen in the observations. The model also reproduces the easterly anomalies to the north and south of this patch, although they are far too weak to the north. The easterly winds in the east Pacific are reproduced by the model. However, these types of models always reproduce easterlies in this region during warm events, even when they are not observed, which is typically the case (Rasmusson and Carpenter 1982).

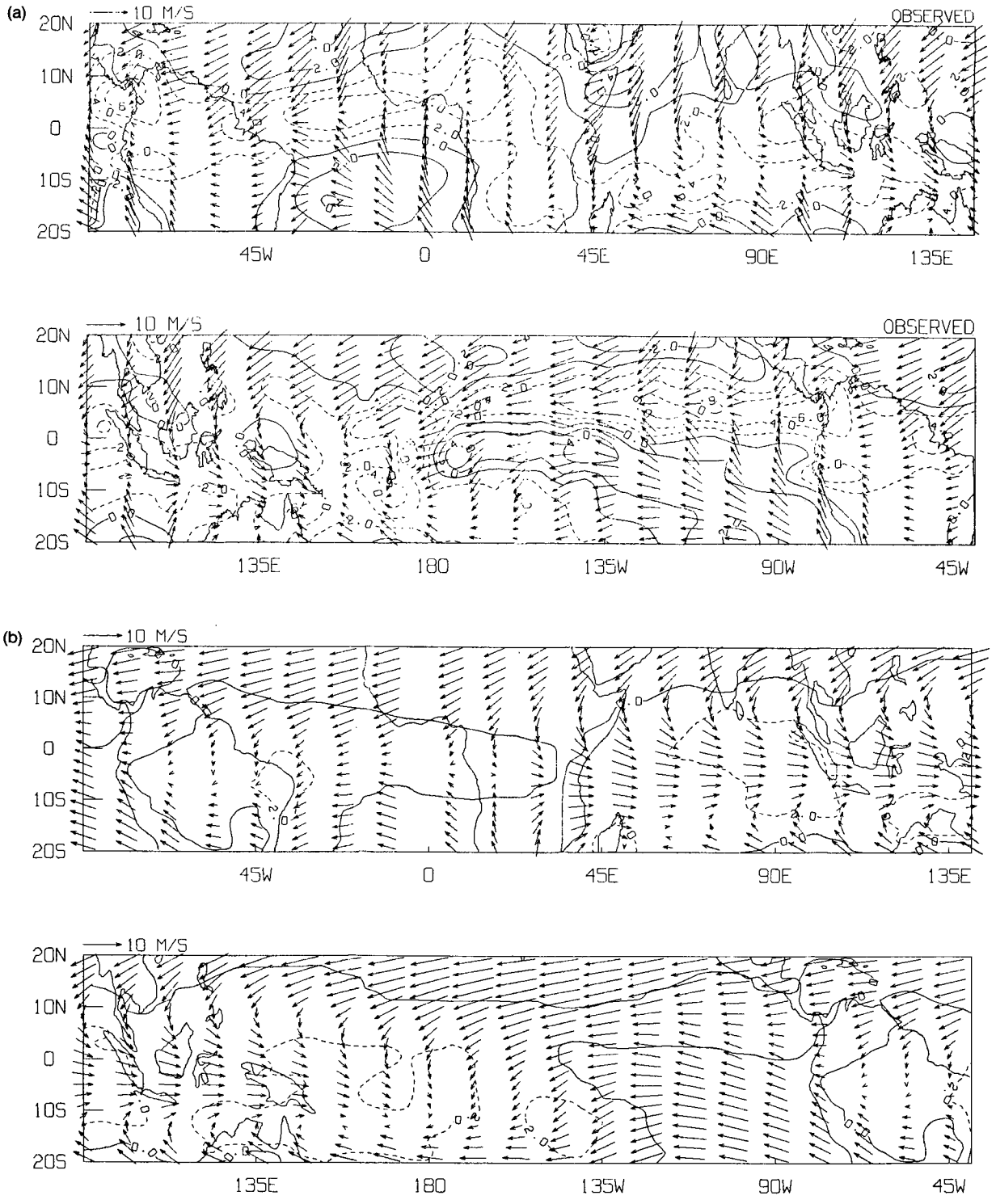

FIG. 3. (a) Observed (after Oort 1983) and (b) model winds and divergence for January. Units are 10^{-6} s^{-1}.

Zebiak (1990) attributes the problem to the fact that parameterizing the atmospheric heating in terms of the SSTA leads to meridionally broad heating, which projects strongly onto a Kelvin wave mode. In nature the anomalous heating has a meridional scale far smaller than that of the SSTA and will therefore project weakly onto the Kelvin wave. January 1987 was atypical in this regard because easterlies were observed over the

east Pacific, and the model agreement may be fortuitious. Easterly anomalies over the Amazon basin are however quite typical of this stage of a warm event, and here the model wind anomalies are in reasonable agreement with observations even though the model anomalies would appear to have a Kelvin wave form. Again, it may be that this is the "right answer for the wrong reasons."

The model precipitation anomaly has a large maximum in the east and central Pacific that is centered

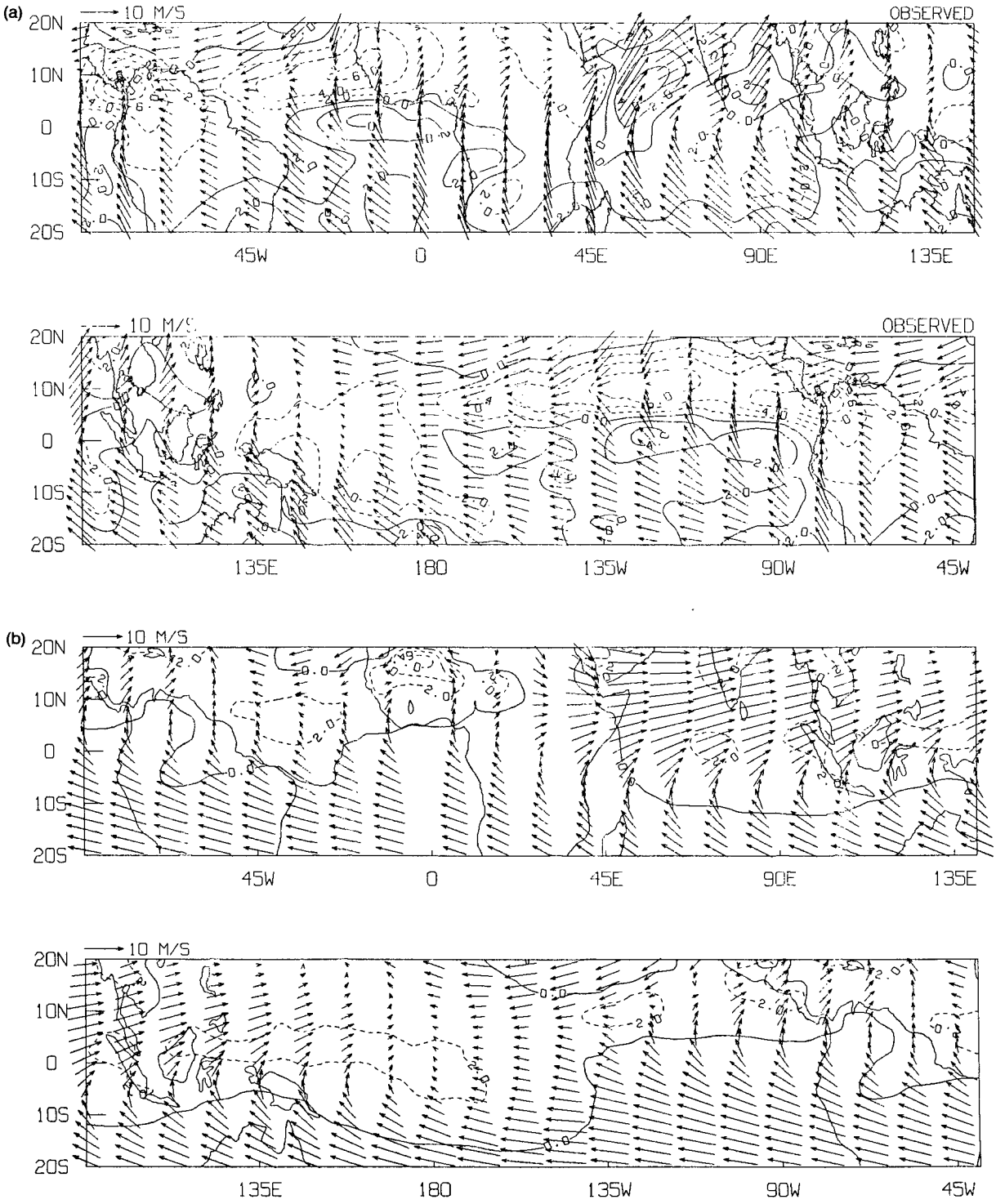

FIG. 4. Same as Fig. 3 but for July.

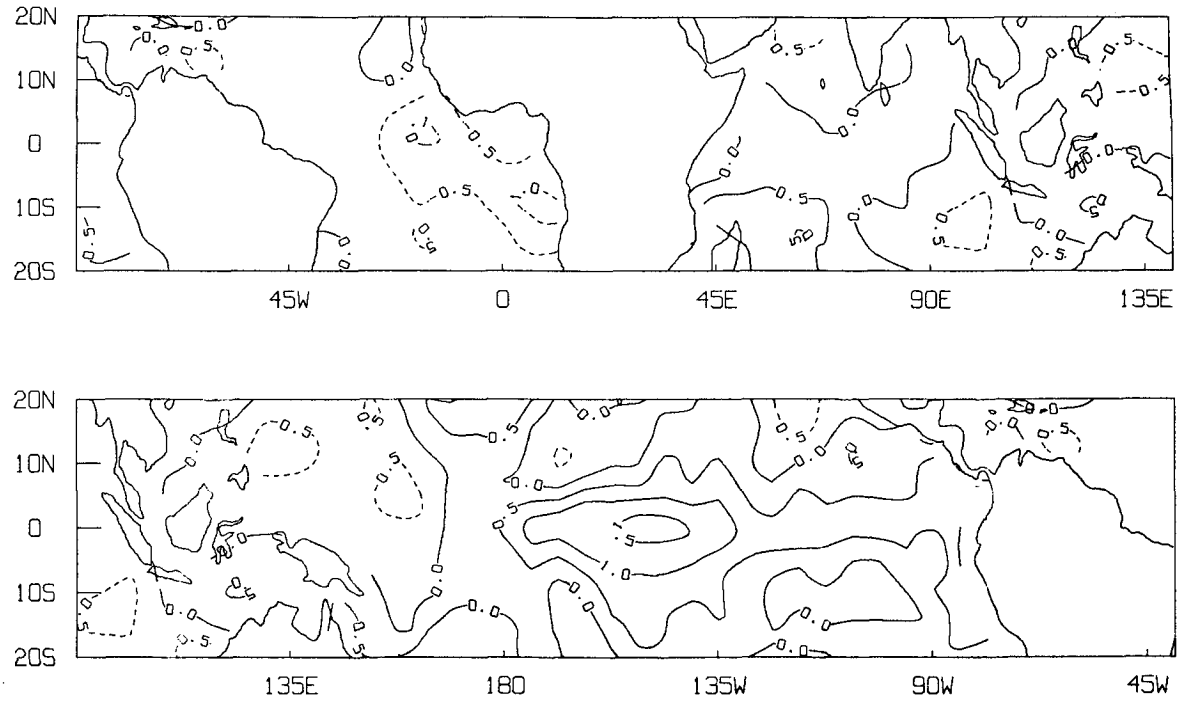

FIG. 5. Observed surface temperature anomaly (°C) for January 1987. Data are from Reynolds (1988).

over the maximum SSTA. If OLR anomalies are assumed to indicate precipitation anomalies, then this maximum should be farther west near the maximum of total, rather than anomalous, SST as shown in Fig. 6. However the regions of negative precipitation anomalies to the northwest and southwest of this main anomaly are in broad agreement with observed OLR anomalies.

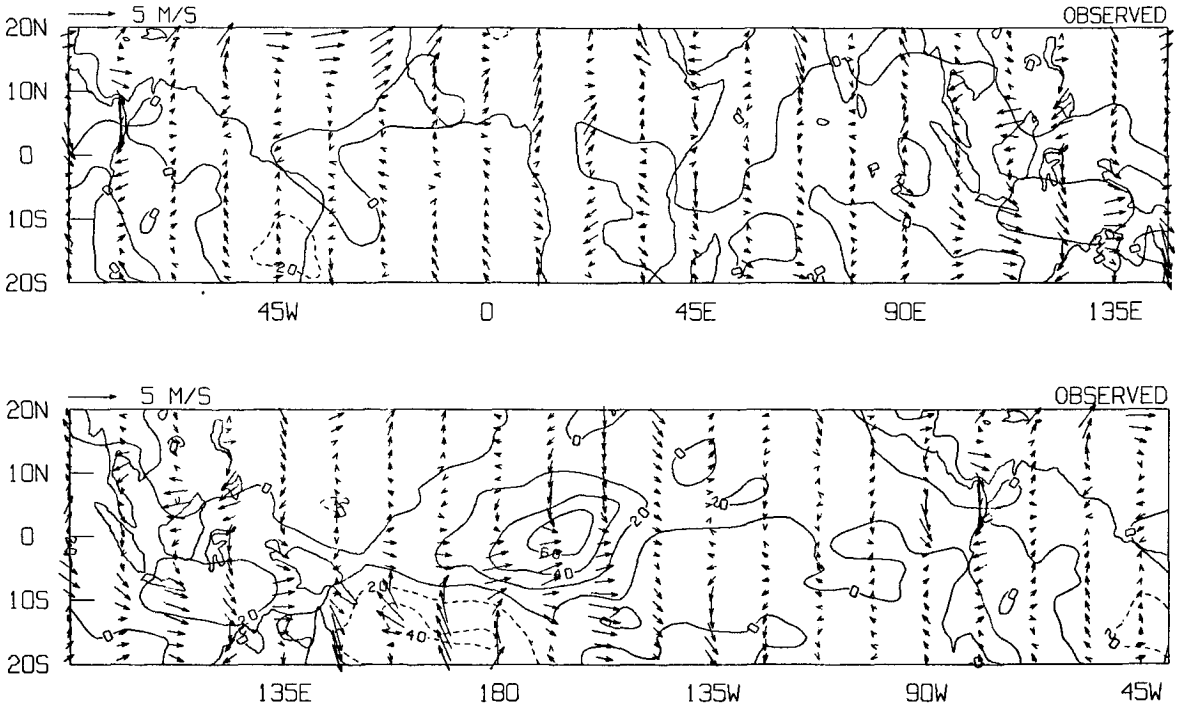

FIG. 6. Observed 1000-mb wind anomalies for January 1987 taken from the NMC analysis and the negative of outgoing longwave radiation anomaly (W m^{-2}).

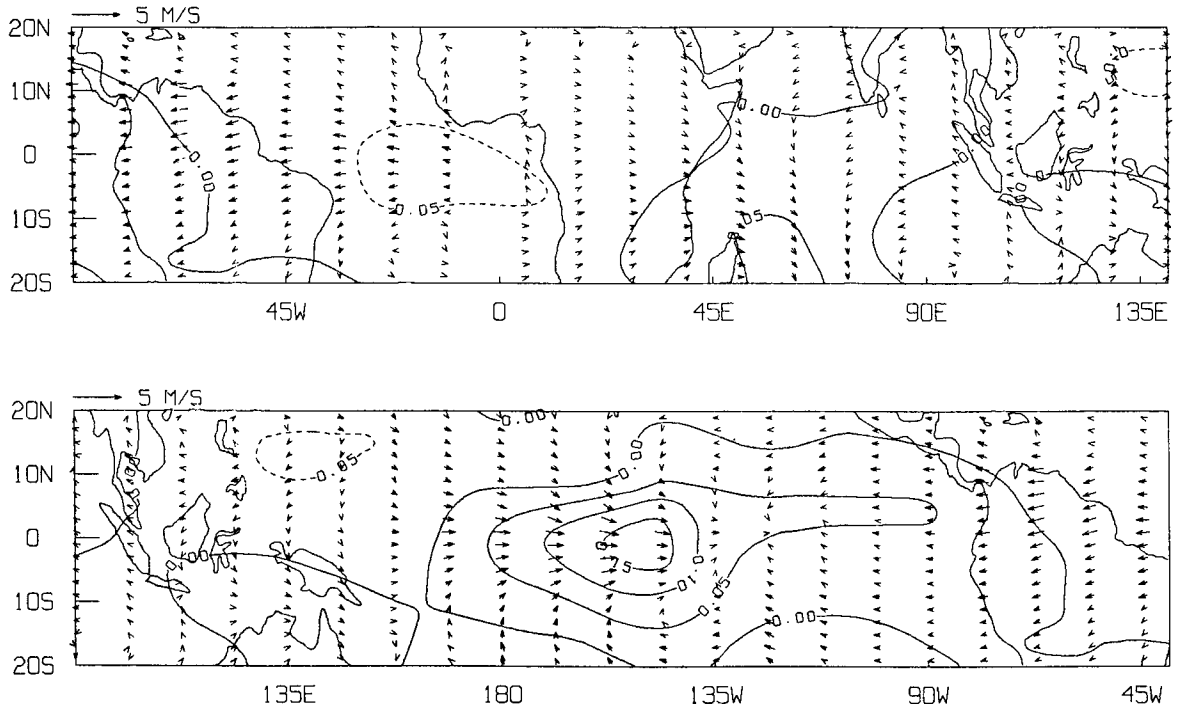

FIG. 7. Model wind and precipitation anomalies for January 1987. Precipitation anomalies are plotted in nondimensional units but the contour interval corresponds to approximately 1.4 mm day^{-1}.

Outside of the Pacific sector there is an area of positive precipitation anomaly over the Indian Ocean and a negative anomaly over the equatorial Atlantic and off northeastern South America. The former agrees quite well with the observed OLR anomaly, but the observations show only a small OLR anomaly off South America. However, the model precipitation anomaly agrees reasonably well with the composite El Niño precipitation anomaly pattern of Ropelewski and Halpert (1987). On the other hand, the observed OLR anomaly for this month is weakly negative over the equatorial Atlantic, even though the SST anomaly here is negative. Interestingly, when an experiment was performed with forcing only in the Pacific sector, the Indian Ocean anomaly essentially disappeared but the South American anomalies remained. Although the South American anomalies were weaker than those generated using SSTAs around the globe, this suggests that the observed precipitation anomalies over this continent are partly forced from the Pacific sector. The tropical Atlantic SSTAs that enhance these precipitation anomalies could in fact be a response to anomalous winds that are generated by anomalous convection over the central Pacific.

Figure 8 presents the SST anomaly for July 1988, which shows a strong cold event in the eastern and central equatorial Pacific. Figure 9 shows the NMC 1000-mb wind anomaly and the negative of the OLR anomaly for this month, and Fig. 10 displays the model wind and precipitation anomaly. The dominant observed feature is the region of enhanced OLR associated with the stronger than normal equatorial cold tongue. The observed wind anomalies in this region are easterly and up to 3 m s^{-1}. There are prominent areas of reduced OLR over the Indian Ocean and maritime continent north of the equator and over the equatorial Atlantic. The first of these two regions is associated with a generally easterly wind anomaly, and the Atlantic region is associated with a westerly anomaly.

The model reproduces many of these features, but the region of enhanced precipitation in the east and central Pacific is too broad in meridional extent and is centered too far east. The model fails to capture the strong easterly flow in this sector south of the equator. Over the Indian Ocean and maritime continent, the model produces a positive precipitation anomaly, but this coincides with westerly, rather than easterly, wind anomalies. In the Atlantic sector, the model creates a positive precipitation anomaly north of the equator but also creates a spurious positive anomaly at about 15°N (where the SST anomaly is positive) and a spurious negative anomaly over West Africa. However, the wind anomalies in this region are reasonably directed.

In both months shown here, the observed wind anomalies are far stronger than those simulated, and the model circulation is smoother and less detailed than observed. The first of these errors is quite disappointing. This model has the problem, common to many models, that since it was designed to simulate total flows, and hence was "tuned" to achieve that, it has difficulty simulating appropriately sized anomalies. The second

error is partly explained by the comparison to monthly, rather than seasonal, means. Monthly means will include higher-frequency phenomena that the model is incapable of capturing that would not necessarily appear in seasonal averages. In addition, strong anomalous flows on the subtropical flanks of the region of interest are quite likely to be forced by extratropical circulations that are absent from the model. A more serious problem is that the model's heating anomalies are too closely related to the SST anomalies, whereas the observations indicate that it is possible to get negative heating anomalies over positive SST anomalies (e.g., over the northern Atlantic in July 1988). The model is quite incapable of reproducing such a relationship.

6. Conclusions

In earlier studies, the Gill model has been used to simulate the total wind field that is forced by imposed atmospheric heating (Webster 1972) or GCM vertical velocities and precipitation (Neelin 1988). A similar model for tropical convergence, but based on assumptions concerning the moist static energy budget, was presented by Neelin and Held (1987). The study presented here is the first attempt to use the Gill model to model total wind fields, rather than departures from climatology or the divergent component only, in a formulation where the model has the ability to determine its own heating. One possible conclusion is that these simple dynamical models are as inadequate in modeling total fields as they are in modeling anomalies. (This conclusion in itself may not be too discouraging, because many features of the total low-level wind field are in fact captured, though with major differences remaining.) Instead, it is suggested that this paper adds to a recent body of work that demonstrates the validity of the *dynamics* contained within the Gill-type model.

It is difficult to have the same qualified confidence in the thermodynamics of the model. Neelin (1988) presented quite reasonable simulations of total low-level flow in a similar model when forced by either GCM vertical velocity or precipitation, and Zebiak (1990) showed it was possible to produce very good anomaly winds for reasonable forcing fields. Both of these results suggest that the problem with simple models lies with their thermodynamics not the dynamics. It is believed that the current model supports that conclusion and that the main source of error lies with the treatment of the atmospheric heating.

If that is so, then the results of the simulations of anomalous circulations shown here are somewhat disappointing, appearing less realistic than those shown in Zebiak (1986). This is despite the greater physical basis for the convective heating parameterization used here than those previously used in similar models and despite the allowance for spatial variations of the moisture field. Zebiak (1986) speculated that the latter would force larger heating anomalies in the western Pacific than in the east because the greater moisture there would intensify the moisture convergence. This would have the effect of relocating maximum atmospheric heating anomalies away from maximum SSTAs towards the area of maximum total SST. This effect

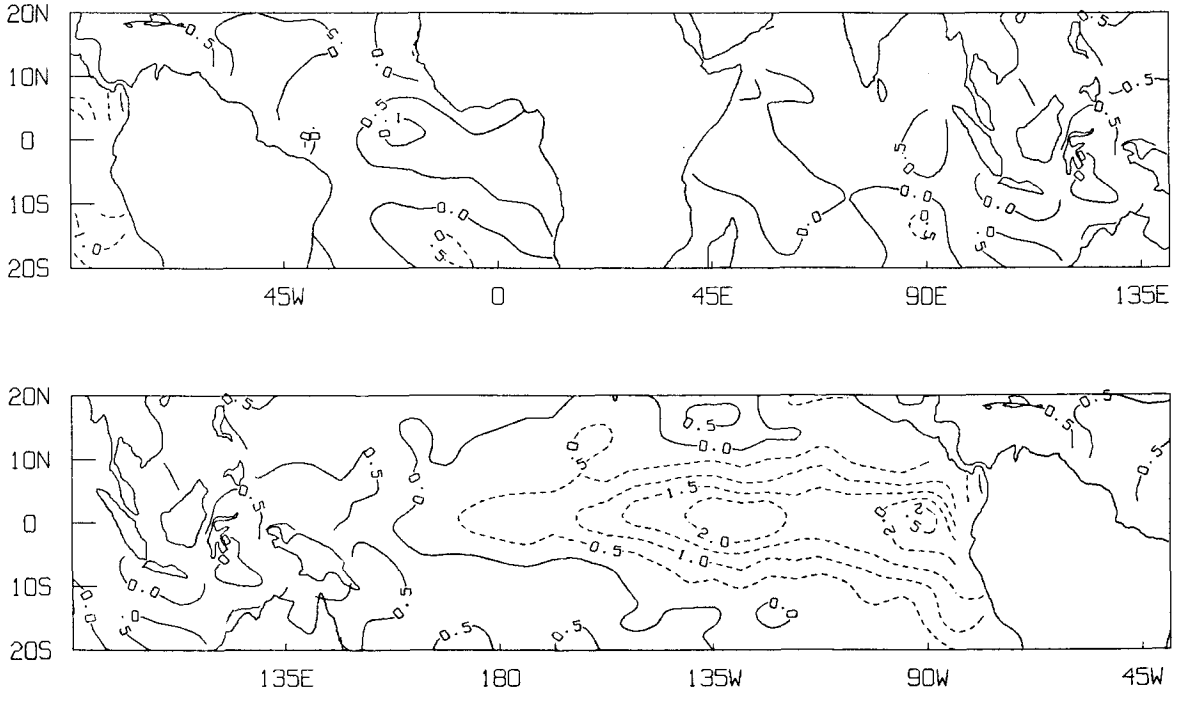

FIG. 8. Surface temperature anomaly (°C) for July 1988. Data are from Reynolds (1988).

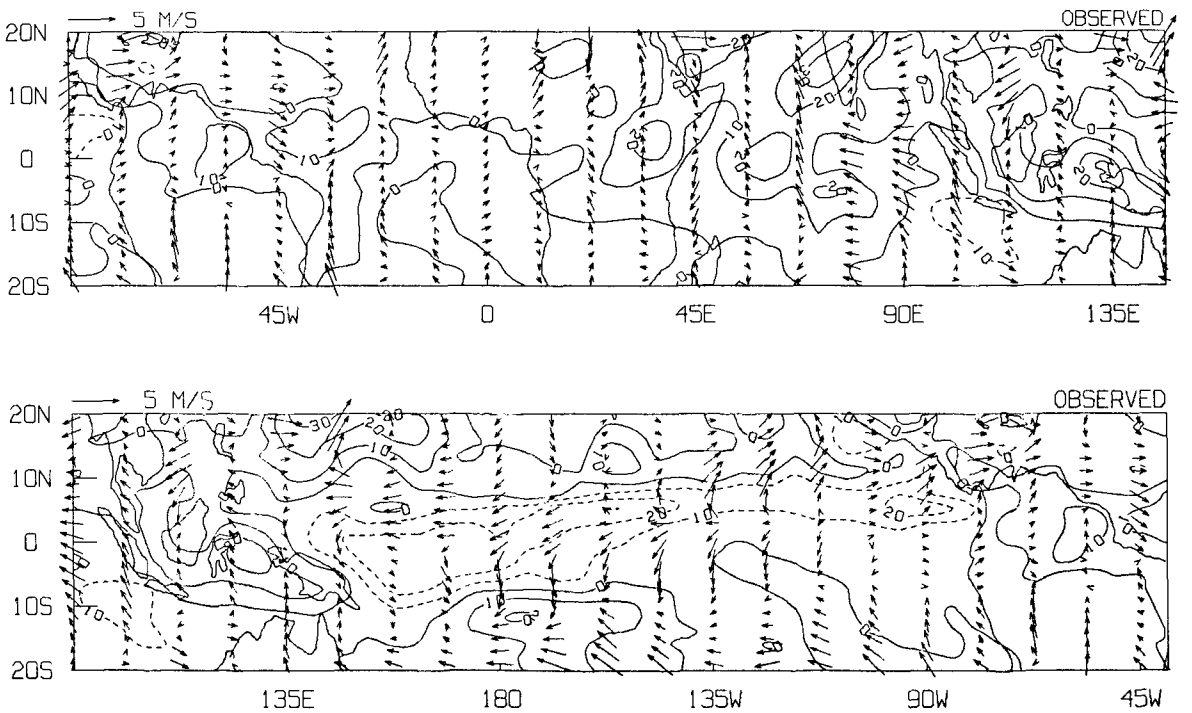

FIG. 9. Observed 1000-mb wind anomalies for July 1988 taken from the NMC analysis and the negative of outgoing longwave radiation anomaly (W m^{-2}).

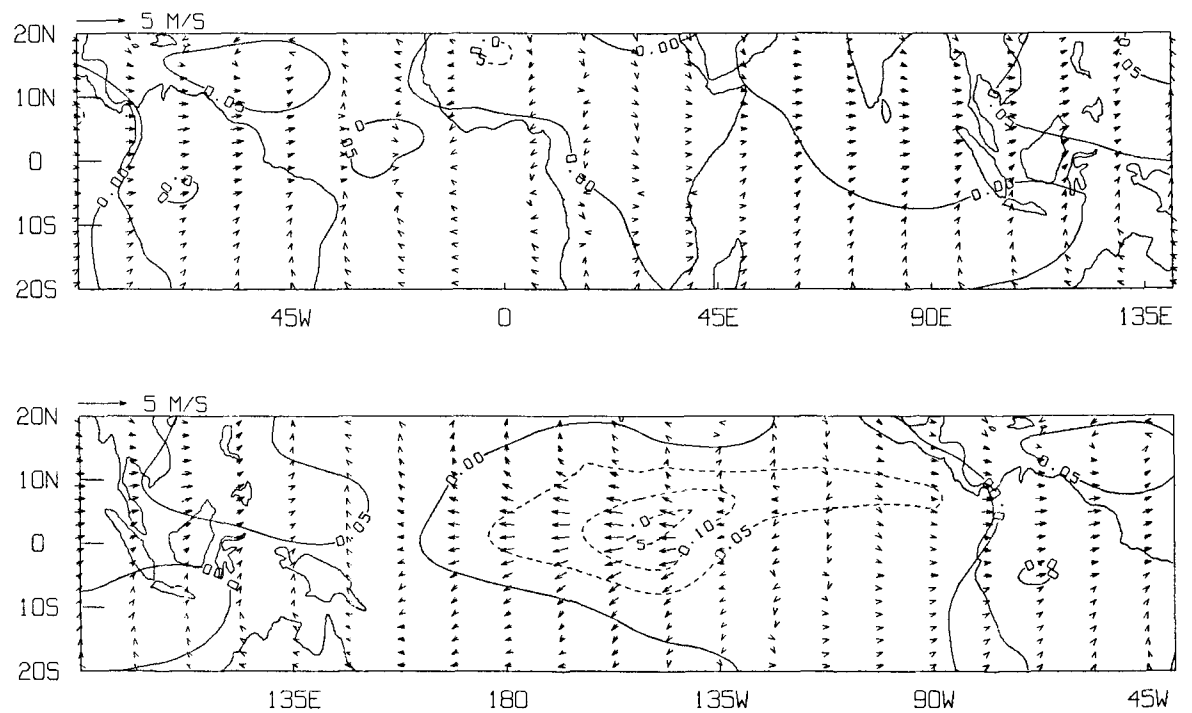

FIG. 10. Model wind and precipitation anomalies for July 1988. Precipitation anomalies are plotted in nondimensional units, but the contour interval corresponds to approximately 1.4 mm day^{-1}.

appears to be overwhelmed in this model, implying that the interaction between the mean and anomaly fields includes greater nonlinearity than simply the nonlinear dependence of saturation moisture content on temperature.

This and other work suggest the following conclusions and directions for further work. Observations of the lower-tropospheric wind field in the tropics show the convergence zones to be very shallow features [in Oort's (1973) dataset, convergence zones are frequently not apparent as low as 900 mb]. Inclusion of an explicit boundary layer is required to capture this. Incorporation of such a layer would also allow inclusion of pressure gradients within the layer created by buoyancy fluxes from the underlying surface. Lindzen and Nigam (1988) have shown these pressure gradients to force, within a model containing the same dynamics as those here, patterns of velocity divergence in qualitative agreement with observations. Some preliminary trials with this kind of forcing produce much sharper and stronger convergence zones than in the current model. Lindzen and Nigam's (1987) model assumes that the convergent mass flux induced by buoyancy fluxes at the surface is taken up by cumulus convection. This, however, bypasses the possibility that cumulus convection, responding to convective instability, can itself induce low-level convergence. This component must be retained and should become more realistic if the areas of deep convection become more limited in extent as a result of inclusion of the boundary layer terms mentioned above.

However, inclusion of surface buoyancy forcing will not solve the whole problem. As shown in Zebiak (1989) areas of atmospheric heating tend to have equally well defined areas of strong atmospheric cooling on their fringes (for example, in the case of the mean circulation these would be to the north and south of the ITCZ). While a model such as the one used here has the meridional resolution to capture this feature, it is not clear that they explicitly contain the required dynamics. This is especially so if, as seems possible, these dipole heating patterns are related to mesoscale circulations, downwelling, and radiative cooling under anvil clouds that spread from the tops of towering cumulus. While some GCMs appear to exhibit similar problems to those seen here—i.e., convergence zones that are too weak and broad—others do not, suggesting that they contain some scale selection process omitted here. It is hoped that whatever this process is the essence of it can be incorporated in a model similar to the one presented here, without a sizeable increase in model complexity.

The assumption of a single mode in the vertical will have to be abandoned. While this mode is a good approximation to the vertical structure of the atmosphere in regions of deep convection, it is considerably less valid away from such areas. For example, in the regions of the subtropical highs adiabatic warming due to descent is balanced by strong radiative cooling to space, but that cooling does not project onto the vertical structure assumed here. It is hoped that a model with the same dynamics, as here but with two deep tropospheric layers and a boundary layer (thus retaining the barotropic mode) and with a slightly more advanced treatment of radiative transfer, will be able to represent the essential physics.

To conclude, here a rather frustrating situation is faced. The feasibility of modeling the total low-level wind field has been demonstrated, and this model can certainly be of use in future studies of the tropical atmosphere system. On the other hand, treatment of heating in the atmosphere seems to be a primary limitation to the realism of these simple models. However, there still remains the challenge of understanding the interaction of convection and the large- (or meso-) scale circulation that determines the structure of atmospheric heating. Future advances in tropical atmospheric modeling will require such a breakthrough.

Acknowledgments. The inspiration for this work came from numerous discussions and *caipirinhas* with Ed Sarachik. I would also like to thank Mark Cane, Steve Zebiak, Rong Fu, Clara Deser, and Mike Wallace for useful discussions and Abraham Oort for prompt provision of the humidity data. This work was supported by National Science Foundation Grant ATM-87-21804.

REFERENCES

Betts, A. K., 1982: Saturation point analysis of moist convective overturning. *J. Atmos. Sci.*, **39,** 1484–1505.

Cane, M. A., S. E. Zebiak and S. Dolan, 1986: Experimental forecasts of El Niño. *Nature,* **321,** 827–832.

Emanuel, K. A., 1986: An air–sea interaction theory for tropical cyclones. Part I. *J. Atmos. Sci.*, **43,** 585–604.

——, 1989: The finite amplitude nature of tropical cyclogenesis. *J. Atmos. Sci.*, **46,** 3431–3456.

Davey, M. K., and A. E. Gill, 1987: Experiments on tropical circulation with a simple moist model. *Quart. J. Roy. Meteor. Soc.*, **113,** 1237–1269.

Findlater, J., 1969: A major low-level air current near the Indian Ocean during the northern summer. *Quart. J. Roy. Meteor. Soc.*, **95,** 362–380.

Gill, A. E., 1980: Some simple solutions for heat-induced tropical circulation. *Quart. J. Roy. Meteor. Soc.*, **106,** 447–462.

Gruber, A., and A. F. Krueger, 1984: The status of the NOAA outgoing longwave radiation dataset. *Bull. Amer. Meteor. Soc.*, **65,** 958–962.

Harrison, D. E., W. S. Kessler and B. J. Giese, 1989: Ocean circulation model hindcasts of the 1982–83 El Nino: Thermal variability along the ship of opportunity tracks. *J. Phys. Oceanogr.*, **19,** 398–418.

Latif, M., 1987: Tropical ocean circulation experiments. *J. Phys. Oceanogr.*, **17,** 246–263.

Lindzen, R. S., and S. Nigam, 1987: On the role of sea surface temperature gradients in forcing low-level winds and convergence in the tropics. *J. Atmos. Sci.*, **45,** 2440–2458.

List, R. J., 1949: *Smithsonian Meteorological Tables.* Smithsonian Institution Press, 527 pp.

Matsuno, T., 1966: Quasi-geostrophic motions in the equatorial area. *J. Meteor. Jap., Ser. II,* **44,** 25–43.

Neelin, J. D., 1988: A simple model for surface stress and low-level flow in the tropical atmosphere driven by prescribed heating. *Quart. J. Roy. Meteor. Soc.*, **114,** 747–770.

——, and I. M. Held, 1987: Modeling tropical convergence based on the moist static energy budget. *Mon. Wea. Rev.*, **115,** 3–12.

Oort, A. H., 1983: Global Atmospheric Circulation Statistics. NOAA Professional Paper No. 14, United States Government Printing Office, Washington D.C., 180 pp. [NTIS PB8-4-129717.]

Philander, S. G. H., and A. D. Siegel, 1985: Simulation of the El Niño of 1982–1983. *Coupled Ocean-Atmosphere Models,* J. Nihoul, Ed., Elsevier Publishers, 517–541.

Rasmussen, E. M., and T. H. Carpenter, 1982: Variations in tropical sea surface temperature and surface wind fields associated with the Southern Oscillation–El Niño. *Mon. Wea. Rev.*, **110,** 354–384.

Reynolds, R. W., 1988: A real-time global sea surface temperature analysis. *J. Climate,* **1,** 75–86.

Ropelewski, C. F., and M. S. Halpert, 1987: Global and regional scale precipitation patterns associated with the El Niño–Southern Oscillation. *Mon. Wea. Rev.*, **115,** 1606–1626.

Seager, R., 1989: Modeling tropical Pacific sea surface temperature: 1970–1987. *J. Phys. Oceanogr.*, **19,** 419–434.

——, S. E. Zebiak and M. A. Cane, 1988: A model of the tropical sea surface temperature climatology. *J. Geophys. Res.*, **93,** 1265–1280.

Shea, D. J., 1986: Climatological Atlas, 1950–1979. NCAR Tech. Note 269+STR, NCAR, Boulder, CO., 35 pp.

Stevens, D. E., and R. S. Lindzen, 1978: Tropical wave-CISK with a moisture budget and cumulus friction. *J. Atmos. Sci.*, **35,** 940–961.

Trenberth, K. E., and J. G. Olson, 1988: An evaluation and intercomparison of global analyses from the National Meteorological Center and the European Center for Medium Range Weather Forecasts. *Bull. Amer. Meteor. Soc.*, **69,** 1047–1057.

Webster, P. J., 1972: Response of the tropical atmosphere to local steady forcing. *Mon. Wea. Rev.*, **100,** 518–541.

Yanai, M., S. Esbensen and J.-H. Chu, 1973: Determination of bulk properties of tropical cloud clusters from large-scale heat and moisture budgets. *J. Atmos. Sci.*, **30,** 611–627.

Zebiak, S. E., 1982: A simple atmosphere model of relevance to El Niño. *J. Atmos. Sci.*, **39,** 2017–2027.

——, 1986: Atmospheric convergence feedback in a simple model for El Niño. *Mon. Wea. Rev.*, **114,** 1263–1271.

——, and M. A. Cane, 1987: A model El Niño–Southern Oscillation. *Mon. Wea. Rev.*, **115,** 2262–2278.

——, 1990: Diagnostic studies of Pacific surface winds. *J. Climate,* **3,** 1016–1031.